THINK INDIA JOURNAL

ISSN:0971-1260
Vol-22- Issue-12-November-2019

Magnetic Properties Of Prussian Blue Analogs Metallo Hexacyanochromates

Sourav Adak

Department of Physics, Lovely Professional University, Phagwara, Punjab 144411, India

Abstract

Magnetization and thermal-expansion studies for Prussian Blue (PB) analogs $M_3[Cr(CN)_6]_2.xH_2O$ (M = *Mn, Fe, Co, Ni*) are reported. Using X-ray diffraction at two temperatures (85 and 300 K), we found evidence that *Fe* and *Co* compounds exhibit large negative thermal expansion effects, while the average thermal expansion coefficient of *Mn* was positive. In this paper, we explore whether thermal expansion and magnetic properties may be correlated. For the *Fe* and *Co* compounds, we determined that effective moments in the paramagnetic range are substantially reduced compared to the values considering free ions. Furthermore, our magnetic studies provide evidence that $Mn_3[Cr(CN)_6]_2.xH_2O$ exhibits long-range magnetic order below ~70 K, while the ground state of the other two compounds is likely paramagnetic.

Copyright ⓒ 2019Authors

ISSN:0971-1260
Vol-22- Issue-12-November-2019

1. Introduction

Negative thermal expansion (NTE) has become the subject of extensive research because of its huge potential for the industrial and technological applications. In particular, it is possible to achieve zero thermal expansion composite materials by using suitable positive and negative thermal expansion materials. Zero-expansion materials are important for many different applications.

NTE behavior is found in select compounds from different classes of materials such as silicates [1], quartz [2], oxides [3,4], zeolites [5] and several other materials. To date, the physical mechanism(s) underlying this phenomenon have often remained elusive, although different models involving molecular dynamics, rigid unit modes, phonon softening, thermal vibrations and guest molecules (for example, H_2O) have had some occasional success. Therefore, understanding NTE behavior in such systems is of interest for basic fundamental research as well.

It has long been known that some Prussian Blue (PB) analogs exhibit large NTE behavior as well. However, not all of the PB analog compounds show NTE and quantitative information is often missing in the literature. PB analogs can be considered as an open-framework material, which offers the possibility to systematically vary the ions. This allows tuning the internal parameters, which in turn may provide insight into correlations between structure and electronic properties. The goal of this work is to explore a possible relationship between thermal expansion and magnetism.

Copyright ⓒ 2019Authors

ISSN:0971-1260
Vol-22- Issue-12-November-2019

We report on the magnetization and the thermal expansion studies of the PB analogs $M_3[Cr(CN)_6]_2.xH_2O$, where $M = Mn, Fe, or\ Co$ and x is the number of water molecules per unit cell. We determined the magnetic ordering temperature (T_{ord}), the paramagnetic Curie-Weiss temperature (θ_p), the effective magnetic moment (μ_{eff}) and the average value of thermal expansion coefficient (α_{avg}).

2. Experimental Methods

Sample Preparation. Powdered materials were obtained using standard chemical precipitation using as-received ACS quality reagents. For synthesis of the PBAs, aqueous solution of metal nitrate was poured into the aqueous solution of potassium chromiumcyanide $K_3[Cr(CN)_6]$ and solid precipitates were filtered, washed with water, dried, and grinded to obtain the powdered material.

The hexacyanochromates of first-row transition metals crystallize in a cubic structure, which consists of octahedra on a cubic lattice connected by cyanide ligands (see Figure 1). The framework structure of our compounds consists mostly of alternating MN_6 and CrC_6 octahedra, but many of the octahedra may be empty and the charge is balanced by guest water molecules on lattice sites or interstitial positions in the unit cell. The number of water molecules in each of the compounds was determined by thermal gravimetric analysis (TGA) using a small fraction of the sample. We found that heating our PB analog compounds to 400^o C leads to complete removal of all water molecules, which in turn destroys the samples.

Copyright ⓒ 2019Authors

ISSN:0971-1260
Vol-22- Issue-12-November-2019

All of our samples had undergone a careful and repeated washing procedure to remove potassium. Potassium hexacyanochromate is soluble in water, and it is one of the reagents used to precipitate the PB analogs. If the reaction does not go to completion, some excess reagents may remain. As a result, the other product of the reaction, besides the PB analog, is potassium nitrate or potassium chloride. Residual excess reagents KNO_3, KCl, or $K_3Cr(CN)_6$ in the final product should not matter, and they should be removable by repeated washing. Moreover, they are simply spectators as far as XRD and magnetic measurements are concerned.

We decided to check the actual potassium content using X-ray fluorescence studies for all three samples after repeated washing. The potassium content in form of the above excess reagents (KNO_3, KCl, or $K_3Cr(CN)$) was estimated to be less than 1% for the two of our PB analogs, namely $Mn_3[Cr(CN)_6]_2.xH_2O$ and $Co_3[Cr(CN)_6]_2.xH_2O$. Somewhat surprisingly, we found that $Fe_3[Cr(CN)_6]_2.xH_2O$ is more problematic and it seems to incorporate K in the PB lattice and not only as spectator reagents. Our XRF studies revealed still a significant amount of potassium (14%) in the $Fe_3[Cr(CN)_6]_2.xH_2O$ PB analog. At present, it is not clear why this PB analog tends to retain K so strongly.

X-ray Diffraction. X-ray diffraction (XRD) patterns at a given temperature under vacuum were obtained via Rigaku Ultima III X-ray diffractometer in Bragg-Brentano geometry with monochromatic CuK_α radiation (λ = 1.54 Å). Rietveld-refinement was performed using General Structure Analysis System (GSAS) software [7] to obtain the lattice parameters and other structural parameters by least-squares fits to the observed

Copyright ⓒ 2019Authors

ISSN:0971-1260
Vol-22- Issue-12-November-2019

diffraction patterns. In order to compute an average thermal expansion coefficient, we performed measurements at two temperatures: at 300 K and at 85 K.

Average coefficient of thermal expansion was computed using the refined lattice parameters with the following formula

$$\alpha_{avg} = \frac{(a_2 - a_1)}{a_1(T_2 - T_1)}, \qquad (1)$$

where a_1 and a_2 are the lattice parameters at T_1 = 85 K and T_2 = 300 K (room temperature), respectively.

Magnetic Measurements. Magnetic studies were performed in magnetic fields up to 14 T in the temperature range 2-300 K. A commercial Quantum Design Physical Property Measurement System (QD-PPMS) was used for the measurements. The experiments were performed using plastic powder capsule used to contain fine particles that are free to rotate in the applied field. That way, one measures the response of the easy-magnetization direction of a material.

3. Results and Discussions

Thermal Expansion Behavior. XRD investigation on $Mn_3[Cr(CN)_6]_2.xH_2O$ had shown that this compound crystallizes in a cubic structure of space group $Fm\ \bar{3}m$ [8]. A sketch of the structure is given in Figure 1. Our room-temperature X-ray diffraction results on *Fe-hexacyanochromate* and *Co-hexacyanochromate* confirm that those two compounds crystallize in the same structure. In general, X-ray diffraction will not provide a good estimate for the location and occupancy of water molecules in the empty spaces between

 Copyright ⓒ 2019Authors

ISSN:0971-1260
Vol-22- Issue-12-November-2019

the octahedra. Water molecules on lattice positions will contribute to the intensities of some Bragg peaks, but there is only weak contribution from the oxygen atoms of the water molecules. Disordered water molecules on interstitial positions, on the other hand, will cause an additional broad hump in the diffraction pattern (see Figure 2). Rietveld refinement provides no means to determine the number of interstitial water molecules, and the hump is fitted as an additional contribution to the background. Accurate values of the lattice parameters were obtained from the refinements, and those are given in table 1. However, in a couple of cases, our lattice parameters seem to be inconsistent with reported values by other authors [9-11]. It should be noted that several parameter may greatly affect the lattice parameters in a particular, such as the actual water content and impurity potassium incorporated in the lattice. As mentioned above, all three compounds contain water molecules after preparation. Using TGA, we determined that the total water content (lattice water plus interstitial water) ranges from 10-14 water molecules per unit cell (see table 1).

Next, we determined the average thermal-expansion coefficient. To do so, we performed additional X-ray diffraction studies at 85 K on the same samples. For the low-temperature study, we used a cold stage and rapid cooling under vacuum. The rapid cooling was needed to prevent water loss. That way, we believe that lattice parameter changes with temperature are intrinsic to the material, and not due to the loss of interstitial water molecules. In Figure 2, we exemplary X-ray data and their refinement for $Co_3[Cr(CN)_6]_2.xH_2O$ at 85 K. Similar experiments were performed for the other two compounds.

Copyright ⓒ 2019Authors

ISSN:0971-1260
Vol-22- Issue-12-November-2019

Using the refined room- and the low-temperature lattice parameters in eq. 1, we then computed an average thermal-expansion coefficient, and those are given in the last column of table 1. The results of our X-ray studies indicate that, averaged between ~85 and 300 K, $Fe_3[Cr(CN)_6]_2.xH_2O$ and $Co_3[Cr(CN)_6]_2.xH_2O$ shows negative thermal expansion while the average coefficient of thermal expansion for $Mn_3[Cr(CN)_6]_2.xH_2O$ is positive.

Magnetic Properties. To explore any possible relationship between magnetism and thermal expansion, we studied magnetic properties of our samples at various temperature and applied magnetic field using the PPMS system described above.

In the inset of Figure 3, we show the temperature dependence of the magnetization. We obtained a value of T_{ord} = 70 K for the magnetic ordering temperature, which is determined from the inflection point in M vs. T plot, in the compound Mn-hexacyanochromate. The *Fe* and *Co* compounds show an increase at much lower temperatures. No saturation tendency was observed to the lowest temperature. Such behavior is reminiscent of the behavior that is commonly observed for a material containing paramagnetic ions and/or magnetic impurities.

In Figure 3, we show as *B/M* which is equal to inverse magnetic susceptibility $1/\chi$. According to modified Curie-Weiss law magnetic susceptibility in the paramagnetic region is given by

$$\chi = \chi_0 + \frac{C}{T - \theta_p}, \qquad (2)$$

where *C:* Curie-Weiss constant and θ_p: paramagnetic Curie temperature. χ_0 is a temperature-independent background term that is often attributed to impurities and

 Copyright ⓒ 2019Authors

ISSN:0971-1260
Vol-22- Issue-12-November-2019

imperfections in the magnetic lattice, which have to be expected in our PB analogs. As can be seen in Figure 3, for all compounds, the modified Curie-Weiss law provides excellent fits of the experimental data.

The relationship between the Curie-Weiss constant *C* and the effective moment in the paramagnetic regime is given by

$$\mu_{eff} = \frac{\sqrt{3k_B C / N_A}}{\mu_B}, \qquad (3)$$

where k_B is the Boltzmann constant, N_A is the Avogardo number and μ_B is the Bohr magneton. Note, that in our case the measured Curie-Weiss constant *C* will have contributions from three M^{2+} and two Cr^{3+} ions per formula unit.

Using eqs 2 and 3, we were able to extract the magnetic parameters for our three compounds: the temperature-independent χ_0 term, the paramagnetic Curie-Weiss temperature, θ_p, and the effective magnetic moment, μ_{eff}. Our results are given in table 2, together with previously reported results, if they exist.

For all three compounds, our fits to the modified Curie-Weiss law (eq. 2) resulted in a negative θ_p, which is an indication of antiferromagnetic correlations. However, only for $Mn_3[Cr(CN)_6]_2.xH_2O$, the fitting results for θ_p were found to be fairly robust, while the θ_p values for the other two compounds were found to vary between negative and positive values depending of the temperature range used in the fits. Since θ_p in $Mn_3[Cr(CN)_6]_2.xH_2O$ is negative, its value is comparable to T_{ord} and the magnetic anisotropy in these cubic materials can be expected to be relatively small, we conclude that this compound orders antiferromagnetically with a Néel temperature $T_N \approx 70$ K.

Copyright ⓒ 2019Authors

ISSN:0971-1260
Vol-22- Issue-12-November-2019

There is no unambiguous evidence of ordering for the other two compounds, and we speculate that their ground states are paramagnetic.

We computed the effective moments from the Curie-Weiss constant *C* and observed that our computed effective moments are somewhat reduced compared to the calculated average values of three M^{2+} and two Cr^{3+} ions for the $Fe_3[Cr(CN)_6]_2.xH_2O$ and $Co_3[Cr(CN)_6]_2.xH_2O$ analogs (see table 2).

Field dependence of the magnetization at different temperatures (2, 10, 20, 50, 100, 200, and 300 K) further corroborate the proposed ground states for the compounds. The results are shown in Figures 4 and 5. The magnetic response of $Mn_3[Cr(CN)_6]_2.xH_2O$ changes around 70 K, below which there is a sudden discontinuous change in the magnetization at low magnetic fields. Unlike the *Mn* compound, the other two compounds exhibit smooth and continuous magnetization curves with a tendency toward saturation in higher fields at all temperatures. This is typical for paramagnetic materials. It should also be noted that we did not find evidence of any ferromagnetic intercept for either compounds, in contrast to previous reports for $Co_3[Cr(CN)_6]_2.xH_2O$ [13]. Figure 5 shows the hysteresis curve for $Mn_3[Cr(CN)_6]_2.xH_2O$ at low temperatures, and it reveals the absence of any remnant magnetization.

4. Conclusion

When one compares the values and signs for the average coefficient of thermal expansion(table 1) with the magnetic parameter values (table 2) for our

Copyright ⓒ 2019Authors

ISSN:0971-1260
Vol-22- Issue-12-November-2019

$M_3[Cr(CN)_6]_2.xH_2O$ Prussian Blue analogs, there seem to be some intriguing hints on possible correlations.

In particular, the *Mn* compound is the only compound that orders magnetically at low temperatures and that shows positive thermal expansion. Secondly, the effective moment of the *Mn* compound is pretty close to the free-ion Mn^{2+} value, while the effective moments for the other two compounds are found to be much more reduced compared to their respective divalent free-ion values. It should be noted, however, that Mn^{2+} has zero orbital moment, while *Fe* and *Co* have orbital momenta. On the other hand, it is reasonable to expect that M^{2+} ions embedded in the octahedral should exhibit fairly localized behavior, i.e. the orbital moment should not be quenched.

In summary, our data may provide some evidence for the following possible correlation between thermal expansion and magnetism. The development of long-range magnetic order and/or localized moments results in regular PTE in PB analogs, while NTE is possible otherwise.

However, the present study explored a small number of compounds only and it was limited to only few physical parameters. Therefore, we cannot exclude at present that apparent correlations happen to be just coincidental. Moreover, our results did not reveal an obvious scaling between any of the magnetic parameters and the thermal expansion coefficient.

Nevertheless, the above studies have shown that it might be worthwhile to explore the possibility of correlations between magnetism and thermal expansion in more detail. Extending studies of possible correlations in a systematic approach to other PB analogs

 Copyright ⓒ 2019Authors

ISSN:0971-1260
Vol-22- Issue-12-November-2019

may help to identify and corroborate potential trends. In addition, we plan to use complementary experimental tools, such as neutron diffraction and scattering techniques, which will test the structural and magnetic properties at a microscopic level.

References

[1] J. G. Collins, G. K. White, Low Temp. Phys. **4**, 450 (1964).

[2] P. R. L. Welche, V. Heine and M. T. Dove, Phys. Chem. Miner. **26,** 63 (1998).

[3] C. Lind, A. P. Wilkinson, Z. B. Hu, S. Short and J. D. Jorgensen, Chem. Mater. **10,** 2335 (1998).

[4] T. A. Mary, J. S. O. Evans, T. Vogt, A. W. Sleight, Science **272,** 702 (2003).

[5] P. Lightfoot, D. A. Woodcock, M. J. Mapple, L. A. Villaescusa and P. A. Wright, J. Mater. Chem. **11**, 212 (2001).

[6] G. L. Harding, P. C. Lanchester and R. Street, J. Phys. C: Solid State Phys. **4**, 2923 (1971).

[7] A. C. Larson and R. B. von Dreele, Los Alamos National Laboratory Report LAUR **86-748** (2000).

[8] H. U. Guedel, H. Stucki and A. Ludi, Inorganica Chimica Acta **7**, 121 (1973).

[9] S. Ohkoshi and K. Hashimoto, Chem. Phys. Lett. **314**, 210 (1999).

[10] E. Coronado, M. C. Giménez-López, T. Korzeniak, G. Levchenko, F. M. Romero, A. Segura, V. Garcia-Baonza, J. C. Cezar, F. M. F. De Groot, A. Milner, and M. Paz-Pasternak, J. Am. Chem. Soc. **130**, 15519 (2008).

 Copyright ⓒ 2019Authors

ISSN:0971-1260
Vol-22- Issue-12-November-2019

[11] W. Kosaka, K. Nomura, K. Hashimoto, and S. Ohkoshi, J. Am. Chem. Soc. **127**, 8590 (2005).

[12] S. Ohkoshi, T. Iyoda, A. Fujishima, and K. Hashimoto, Phys. Rev. B **56** (18), 11642 (1997).

[13] R. M. Bozorth, H. J. Williams, and D. E. Walsh, Phys. Rev. **103** (3), 572 (1956).

Tables and table captions

Table 1

Lattice parameter, *a*, water content (from TGA), *x*, and average values for the thermal expansion coefficient, (α_{avg}), for $M_3[Cr(CN)_6]_2.xH_2O$ (M = Mn, Fe, Co and Ni).

The average coefficient of thermal expansion(CTE) was computed from the refined lattice parameters at 85 and 300 K, obtained from Rietveld refinement with GSAS.

Compound	Lattice const. [ ] at RT	Water content, x	α [10^{-6} K^{-1}]
$Mn_3[Cr(CN)_6]_2.xH_2O$	10.892(3)	12	27.0 ± 2.2
$Fe_3[Cr(CN)_6]_2.xH_2O$	10.1486(27)	10	-
			19.7 ± 1.8
$Co_3[Cr(CN)_6]_2.xH_2O$	10.2387(13)	14	-9.8 ± 5.7
$Ni_3[Cr(CN)_6]_2.xH_2O$	9.9811	16	4.0 ± 10.6

Copyright ⓒ 2019Authors

ISSN:0971-1260
Vol-22- Issue-12-November-2019

Table 2

Magnetic parameters of $M_3[Cr(CN)_6]_2.xH_2O$ (M = *Mn, Fe, Co,* and *Ni*). T_{ord} denotes the magnetic ordering temperature, χ_0 the temperature-independent susceptibility term, θ_p the paramagnetic Curie temperature and μ_{eff} the effective magnetic moment determined in the paramagnetic region. The calculated average values for the full moments (spin and orbital) for divalent M^{2+} and trivalent Cr^{+3} are listed as well. For comparison, previously published data are also included.

Compound	T_{ord} [K]	χ_0 [10^{-8} m^3/mol]	θ_p [K]	μ_{eff} [μ_B]	calculated average moment [μ_B]	ref.
$Mn_3[Cr(CN)_6]_2.12H_2O$	70.0 (T_N)	8.32(6)	-52.21(39)	5.3	5.1	this study
	67.0 (T_C)		-54.00			[12]
$Fe_3[Cr(CN)_6]_2.10H_2O$	-	4.41(0)	-2.26(02)	3.4	5.6	this study
$Co_3[Cr(CN)_6]_2.14H_2O$	-	1.22(1)	-11.02(04)	4.6	5.5	this study
	13.0 (T_C)			4.2		[13]
$Ni_3[Cr(CN)_6]_2.16H_2O$		0.80(1)	18.15(4)	2.8	3.3	this study

Copyright ⓒ 2019Authors

ISSN:0971-1260
Vol-22- Issue-12-November-2019

Figure Captions

Figure 1

Structure of PB analogs metallo-hexacyanochromates $M^{II}_3[Cr^{III}(CN)_6]_2.xH_2O$. Not all of the octahedra are occupied by ions, and water molecules are present on lattice or interstitial positions between the octahedra.

Figure 2

Calculated (line), observed (symbols) and difference profile (grey line) for cobalt hexacyanochromate, $Co_3[Cr(CN)_6]_2.xH_2O$, at 85 K.

Figure 3

Reciprocal molar susceptibility $(1/\chi)$, measured as B/M, as a function of temperature. The lines indicate the modified Curie-Weiss fit above ~100 K for all the compounds. The fitting parameters are listed in table 2. Note that the lines for the *Fe* and *Co* compounds are on top of the symbols over the whole temperature range. The inset shows the magnetization as function of temperature.

Copyright ⓒ 2019Authors

ISSN:0971-1260
Vol-22- Issue-12-November-2019

Figure 4

Magnetization as a function of field for the $M_3[Cr(CN)_6]_2.xH_2O$ *(M = Mn, Fe, Co, Ni)* compounds, measured at various fixed temperatures (2, 10, 20, 50, 100, 200, and 300 K).

Figure 5

Hysteresis loop for the PB analog $Mn_3[Cr(CN)_6]_2.xH_2O$ at 5 K.

Copyright ⓒ 2019Authors

ISSN:0971-1260
Vol-22- Issue-12-November-2019

Figures

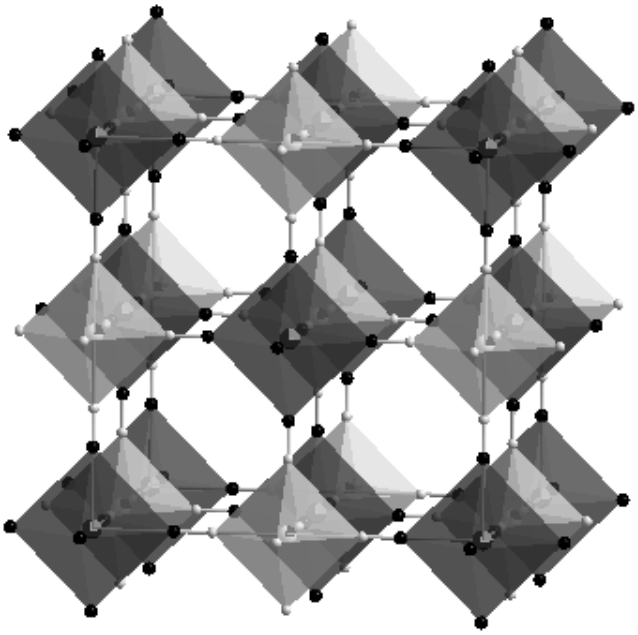

Figure 1

Copyright ⓒ 2019Authors

ISSN:0971-1260
Vol-22- Issue-12-November-2019

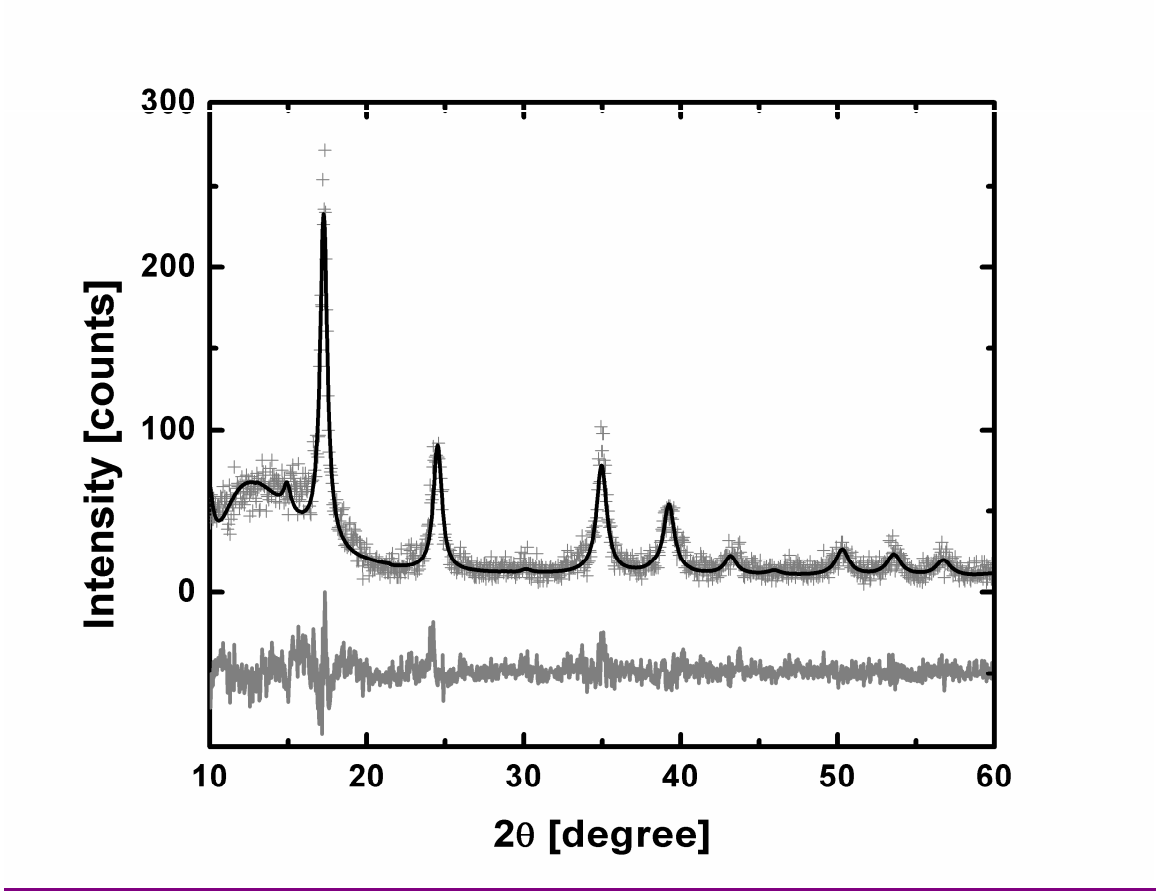

Figure 2

Copyright ⓒ 2019Authors

ISSN:0971-1260
Vol-22- Issue-12-November-2019

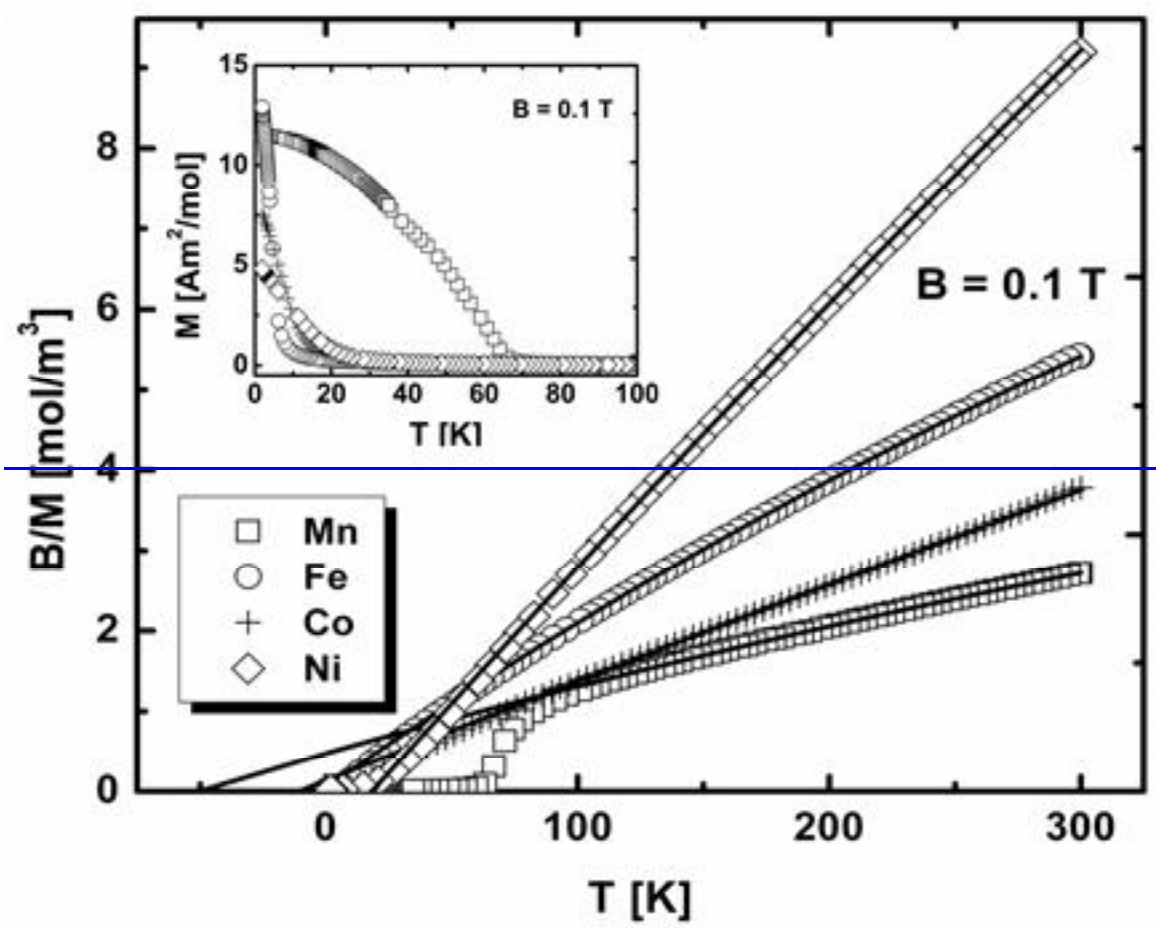

Figure 3

Copyright ⓒ 2019Authors

ISSN:0971-1260
Vol-22- Issue-12-November-2019

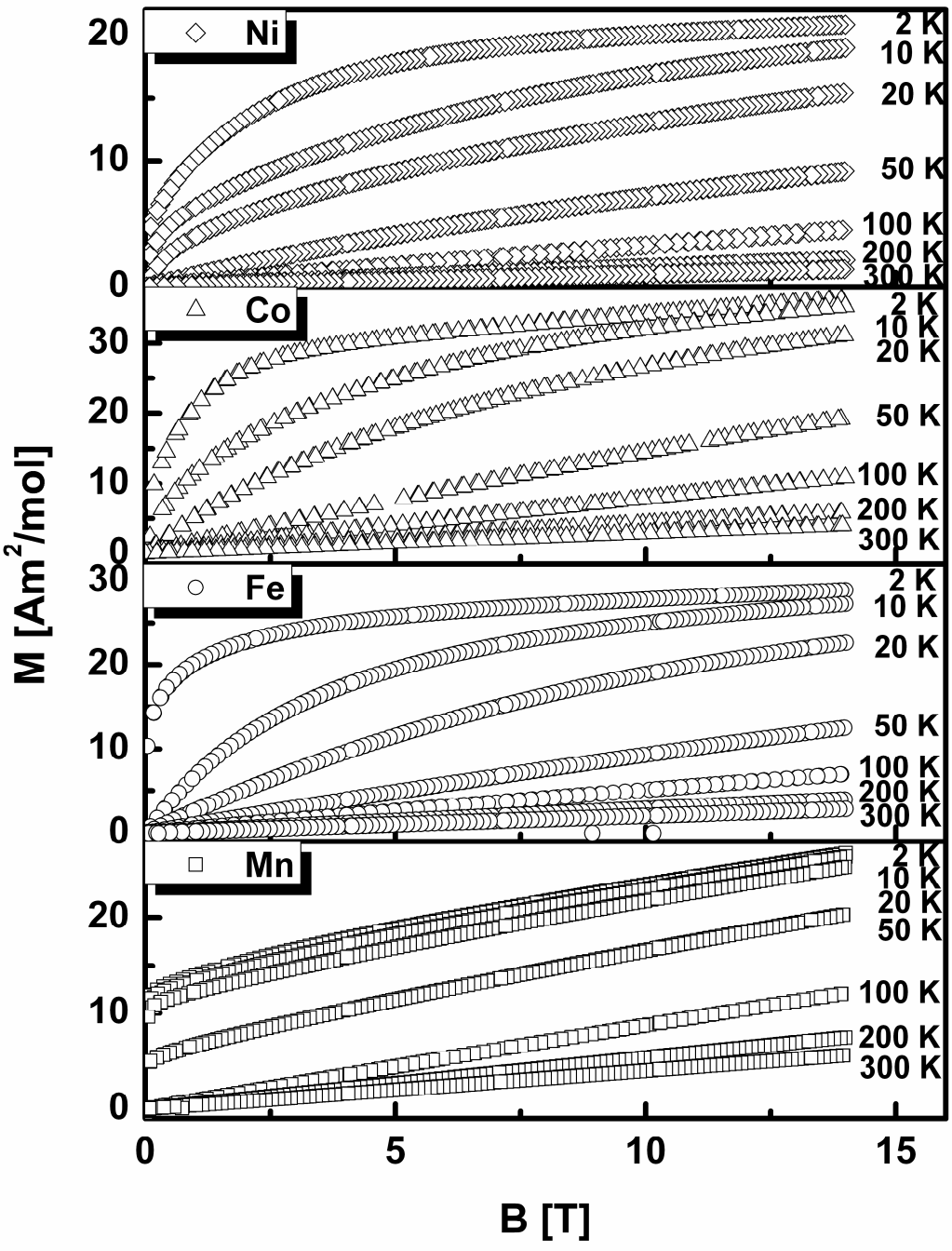

Figure 4

Copyright ⓒ 2019Authors

ISSN:0971-1260
Vol-22- Issue-12-November-2019

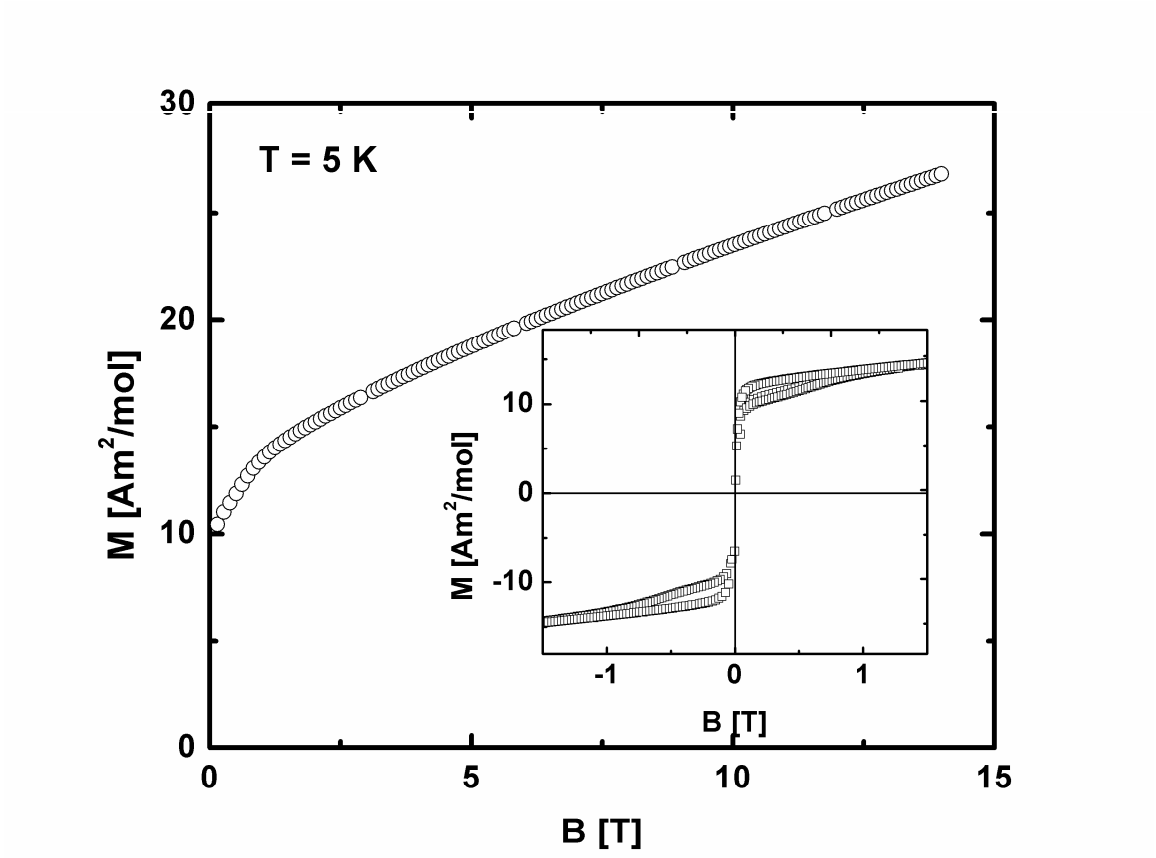

Figure 5

Copyright ⓒ 2019Authors